

An approach of the internal friction-dependent temperature changes for conventional and pure biogenic lubricating greases

Leif AHME^{1,*}, Erik KUHN¹, Miguel Ángel DELGADO²

¹ Department of Mechanical Engineering and Production Management, Hamburg University of Applied Sciences, Hamburg 20099, Germany

² Department of Chemical Engineering, Research in Product Technology and Chemical Processes (Pro2TecS), University of Huelva, Huelva 21071, Spain

Received: 17 December 2022 / Revised: 25 May 2023 / Accepted: 27 August 2023

© The author(s) 2023.

Abstract: This work investigated the temperature changes inside the bulk of lubricating greases under controlled high-shear stress conditions (250–500 s⁻¹). For this purpose, a newly developed temperature-measuring cell called Calidus was successfully tested. The temperature changes (ΔT) have been related to the greases' components (thickener, base oil-type, and composition) and the structural degradation of the lubricating greases. Furthermore, a theoretical approach was proposed for calculating the internal temperature change of lubricating greases during shear stress. All greases showed an internal temperature profile characterised by a sudden rise in ΔT within the first 4 h from starting the test and subsequent ΔT decay until it reaches the steady state value. Furthermore, it was found that greases C1 and C5, formulated with lithium and calcium soap, respectively, with different soap content (16.1 wt% and 9.7 wt%, respectively), but the same base castor oil, showed the highest value of the maximum ΔT , c.a. 3.2 K, and the most drastic drop of ΔT . These greases showed both the highest specific densities and heat capacities. In addition, they showed the lowest ratio of expended energies (R_{tee}), which means more structural degradation in the stressed grease. On the contrary, the grease C3, with 13 wt% of Li-soap but the lowest base oil's viscosity, showed the lowest maximum ΔT and the temperature profile was characterised by a moderate variation of ΔT along the test. The biogenic grease B3 developed a low-temperature change in the group of pure bio-genic greases close to grease C3.

Keywords: shear-induced structural degradation; rheology; temperature measurements; lubricating greases density; lubricating greases specific heat capacities

1 Introduction

The primary function of lubricants is to reduce friction and wear [1]. In addition, cleaning, sealing, and cooling functions used to be assigned to lubricants in different degrees depending on whether they are lubricating oils or greases. Lubricating greases consist of base oil and a thickener, among other additives. It is a colloidal suspension where the thickener forms a three-dimensional (3D) structure (gel-like) inside the base oil, adding a significant viscoelastic characteristic [2]. Lubricating greases generally

consist of 65 wt%–95 wt% base oil (mineral oil, synthetic oil, or vegetable oil), 5 wt%–35 wt% thickener, and 0–10 wt% additives [1]. They are used when applying lubricating oils is technically or economically disadvantageous or impossible [3]. Lubricating greases are mainly used in ball bearings under mixed friction conditions. Different researchers [4–7] have investigated the tribological and rheological behaviour of lubricating greases with different approaches.

An ongoing problem in tribology is the behaviour of grease under lubrication conditions, or in other words, the effect of viscoelasticity on the friction

* Corresponding author: Leif AHME, E-mail: leif.ahme@haw-hamburg.de

Nomenclature

c_{pi}	Sample specific heat capacity (J/(g·K))	T_0	Starting temperature value (K)
M_d	Measured Torque (N·m)	T_i	Measured temperature value (K)
m_i	Sample mass (g)	U_1-U_2	Change in the internal energy of a closed system (J)
n	Rotational velocity (min ⁻¹)	V_i	Sample volume (cm ³)
NLGI	National Lubricating Grease Institute	W_{12}	Amount of thermodynamic work done by the system (J)
PAO	Poly-alpha-olefin	ΔT	Temperature change (K)
Q_{12}	Quantity of energy supplied to the system as heat (J)	ρ_i	Sample specific density (g/cm ³)
R_{tee}	Ratio of the total expended energy		
R_z	Average surface roughness		

process. One way to clarify this problem is to determine the rheological properties of lubricating greases. Lubricating greases are exposed to structural degradation due to frictional stress, which can be divided into mechanical and chemical degradation. Delgado et al. [8] and Kuhn [9] have already attempted to analyse the lubricating grease-based friction process by rheological measurements. Kuhn [10] described that friction could be understood as the input (storage) and output (loss) of energy in the tribo-system, and wear may be related to the dissipation of this energy. Other researchers [7, 10–14] have used a thermodynamic approach to describe grease structural degradation better. In this regard, Bryant et al. [14] defined the generalised thermodynamic and degradation forces ratio as the term “degradation coefficient” for the first time. The calculation was based on the entropy concept and the degradation process instead of process variables. Rezasoltani and Khonsari [6] characterised the structural degradation of greases by showing that the shearing process breaks down the grease structure and leads to heat production. Entropy is generated during the heat transformation caused by the structural degradation process. From a thermodynamic point of view, Rezasoltani and Khonsari [6] and Osara and Bryant [12] described the degradation coefficient as a correlation of the entropy generation rate with mechanical degradation. Nevertheless, most of these studies focus on the numerical treatment of heat generation due to the mechanical degradation of greases. Kuhn [15] studied the specific entropy transport using different temperature values, such as the maximum

friction energy temperature and the fixed temperature chamber. For further investigations according to Kuhn’s model, it is helpful to know how greases behave regarding the temperature in the grease film.

It is known that temperature highly influences the viscosity and viscoelasticity of greases [16]. Various works on temperature investigations have different approaches, but in most cases, the heat is transferred externally into the system [13, 17–20]. For lithium lubricating greases, Delgado et al. [17] determined a critical temperature of 110 °C in their investigations, at which the viscoelastic behaviour of Li-greases drastically decayed. Pan et al. [18] concluded that after short thermal ageing at 120 °C for 2–24 h of lubricating greases, the high interconnections of the network microstructure and, in particular, the strength of the fibrous structure decrease. In addition, they pointed out that the interpretation of its chemical composition did not cause the variation in the lubrication performances after that short heat treatment but by its physical entanglement strength. With the help of a homemade Couette ageing machine, Zhou et al. [20] have developed a master curve for grease ageing. They showed the influence of temperature and shear on the mechanical ageing of lubricating greases with a fibrous-based structural skeleton. They observed that an increase in temperature accelerated the shear degradation. Rezasoltani and Khonsari [13] have developed a model examining greases at different shear rates and temperatures. This model uses the expressed entropy generation to predict the reduction of grease consistency subjected to mechanical shear.

They restricted themselves to temperatures of 25–45 °C to prevent chemical degradation or evaporation of the base oil. Thus, mechanical degradation is the dominant degradation process in the mentioned model. Only Osara and Bryant [19] studied differentiated temperature measurements to perform a pure heat analysis to evaluate the thermal entropy generation. They combine the fundamental thermal energy and thermodynamics with the degradation entropy generation theorem. For this purpose, they used the results of their study [12], in which they carried out unique temperature measurements by a motorised paint mixer (stirrer) and three thermocouples mounted at different points within the mixing vessel to record the temperature under shearing conditions.

The primary purpose of this work was to investigate the temperature changes inside the bulk of lubricating grease under controlled shear stress conditions (mechanical energy) at room temperature. This investigation focused solely on lubricating greases, not lubricating pairings, since in a mixed regimen, the friction energy is attributable to both the solid and the fluid friction. For this reason, rheometer measurements were chosen to provide accurate information on the fluid friction behaviour of greases. A standard rotational rheometer-measuring cell and a newly developed temperature-measuring cell called Calidus were used. Calidus device makes it possible to determine the temperature profile within the measuring gap. In addition, the basic design of Calidus helps to better isolate the internal temperature measurements from the geometry concerning heat conduction. The obtained results should provide information about the temperatures in the lubricating grease and later be used in a calculation model. In

addition, the temperature change was related to the greases' components (thickener, base oil-type, and composition), and a comparison was made with the structural degradation of the lubricating greases. This work does not consider other influences, such as physico-chemical interactions among components. It allows the quantification of dissipation energy, converted via mechanical energy into thermal energy, and a gradient of intrinsic energy.

2 Materials and experimental methods

2.1 Materials

In this experimental study, ten different grease samples were tested, differing in their composition. They were kindly supplied by Fuchs Europe Schmierstoffe (Mannheim, Germany) and Fuchs Lubritech (Kaiserslautern, Germany). They can be grouped into two groups: On one hand, conventional greases based on lithium soap, calcium soap, and polyurea; on the other hand, newly developed, pure biogenic greases. The composition of the different lubricating greases analysed, and their basic properties are listed in Tables 1 and 2, respectively.

Samples C1–C7 are model lubricating greases with conventional thickeners. These greases were prepared to combine with different types of thickeners and types and viscosities of base oils, according to the study by Delgado et al. [21], as these parameters significantly influence the microstructural skeleton and the rheological behaviour. All of them have an NLGI grade 2, which is why the soap concentration of the greases varies. Although the soap concentration changes the consistency of the greases, its influence

Table 1 Composition and primary technical data of conventional lubricating grease samples studied.

Lubricating greases	NLGI-grade	Thickener type	Thickener concentration (%)	Base oil	Base oil viscosity at 40 °C (mm ² /s)	Dropping point (°C)
C1	2	Lithium-12-hydroxystearate	16.1	Castor oil	240	~190.111
C2	2	Lithium-12-hydroxystearate	10.6	PAO	240	~210.497
C3	2	Lithium-12-hydroxystearate	13	PAO	48	~208.479
C4	2	Lithium-12-hydroxystearate	9.5	Mineral oil	240	~206.493
C5	2	Calcium-12-hydroxystearate	9.7	Castor oil	240	~142.055
C6	2	Calcium-12-hydroxystearate	22.8	PAO	240	~150.872
C7	2	Polyurea	19.6	PAO	240	~296.913

Table 2 Composition and primary technical data of biogenic lubricating grease samples studied.

Lubricating greases	NLGI-grade	Thickener type	Thickener concentration (%)	Base oil	Base oil concentration (%)	Base oil viscosity at 40 °C (mm ² /s)	Dropping point (°C)
B1	1	Cellulose	1.5	Glycerine	88.5	227.4	<≈100?
				Glyceryl-monooleate	10	120.1	
B2	0-1	Polyhydroxy butyrate Ethylcellulose	5.3 7.7	MCT oil	55	14.7	≈80
				Castor oil	22	258.3	
				HOSO	10	46.2	
B3	00	Beeswax Glycerol monostearate Cetyl alcohol	7 5 2	HOSO	50	46.2	≈45
				Castor oil	36	258.3	

on the rheological behaviour is proportional and can be controlled [21]. Samples B1–B3 are biogenic lubricating greases previously tested as part of the TriBioGen research project by Acar et al. [22, 23]. In all cases, no additives were added deliberately to exclude other possible effects on the temperature behaviour.

2.2 Methods

2.2.1 Determination of the density and the specific heat capacities

The specific densities were determined both experimentally and theoretically. However, the specific heat capacities were determined experimentally only because theoretical values could not be sourced for all greases.

The specific densities were experimentally obtained using a PNR 10 penetrometer crucible (Petrotest, Germany) with a defined volume of 3,178 mm³ and a precision balance, model 1602 MP8 (Sartorius, Germany). All samples were tempered with the penetrometer crucible in an F3 S circulating thermostat water bath (Haake, Germany) at 20, 40, and 80 °C for 15 min. After heating, the crucible was drawn off evenly and afterwards, immediately, the weight of the filled crucible was determined. The specific heat capacities were determined using a differential scanning calorimeter (DSC), model DSC 204 F1 (Netzsch, Germany), under a nitrogen atmosphere. Nitrogen flow was maintained at 20 mL/min. Grease samples (16.9–20.9 mg) were placed in closed aluminium crucibles and heated from –40 °C to max. 300 °C, at a heating rate of 10 K/min. At least three repeats of

each test were obtained on fresh samples, and the data shown have statistically significant values, i.e. they did not exceed a significance level of 0.05 on the Student's t-test and had a 95% confidence interval. The specific values were determined by applying the standard protocol described by DIN 51007 [24]. For this purpose, an equation in which the heating rate and the weight of the sample are significant was applied to three measurements performed in the same way (baseline, sapphire, and sample) [25]. A sapphire from a DSC standard set from Netzsch, with a diameter of 4 mm and a height of 0.5 mm, was used for the measurements.

2.2.2 Rheological measurements

To investigate the temperature change inside the bulk of grease, stress-growth rheological tests were performed under controlled shear rate conditions using a smooth cone-plate geometry of 50 mm diameter, coupled to a controlled-stress rheometer model MCR 302 (Anton Paar, Austria). The measuring device was supplemented with an environmental control chamber (bonnet) to prevent external influences such as heat loss due to draughts or other environmental influences. According to the ISO 3219-2 standard, a cone angle of 1° was used. The gap resulting from the measuring system was always 0.103 mm. Shear test conditions of greases on the rheometer may deviate considerably from actual operating conditions but still provide a practical measure of the shear-induced frictional energy of the grease under shear stress. As Kuhn [2] and Delgado et al. [26] pointed out, adverse phenoms such as wall slip and leakage may be produced during rotational tests, significantly affecting the rheological results.

Thus, a cone-plate geometry was selected because it lets uniform shear conditions in the entire conical gap. Furthermore, a small sample size is required, allowing for better temperature measurement.

The experimental procedure with rheometers was organised in two consecutive steps (Fig. 1). The torque, rotational speed, and temperature were recorded every 15 s during the rheological measurements (5,320 points were recorded). It was done to quantify how much energy was introduced into the tested grease volume and how the internal frictional energy evolved along the test. In addition, it enables a statement about the temperature behaviour of the lubricating greases and the mechanical stress following the measurements.

In the first test step, the sample was stressed with a short linear shear rate ramp from 0 to the maximum values of 250 and 500 s^{-1} for 600 s. These shear rates selected in this series of tests were based on DIN 51810-1 [27]. In order to avoid material leakage in the measuring gap, it was decided not to use shear rates higher than 500 s^{-1} . The short linear shear rate ramp of 600 s was deliberately chosen to avoid possible leakage effects due to a sudden high shear rate. The temperature change in the bulk grease was recorded directly at the start of the measurement. In the second phase, the sample was stressed at a constant shear

rate (250/500 s^{-1}) for 79,200 s to record both a long period of temperature change and, simultaneously, to induce structural changes in the lubricating greases under liquid friction-liked conditions. Three replicates were performed on fresh samples for each grease. Afterwards, a mean value was calculated for all three outcomes.

2.2.3 Temperature measurements

Different temperature environments can be simulated during the rheological tests, and the reference temperature can be kept constant or dynamic. However, the behaviour differs at a given temperature than under real conditions, i.e., non-constant temperature conditions. As an innovation in this research work, internal temperature measurements within the bulk grease were recorded during the structural degradation behaviour of greases, which was investigated in rheological tests. It allows the quantification of dissipation energy, converted via mechanical energy into thermal energy and a gradient of intrinsic energy.

This work chose two different approaches to record the temperature values during the stress-growth test. Firstly, a standard plate Peltier temperature control system (PTD) from Anton Paar (Fig. 2) was used. In this configuration, the temperature sensor was

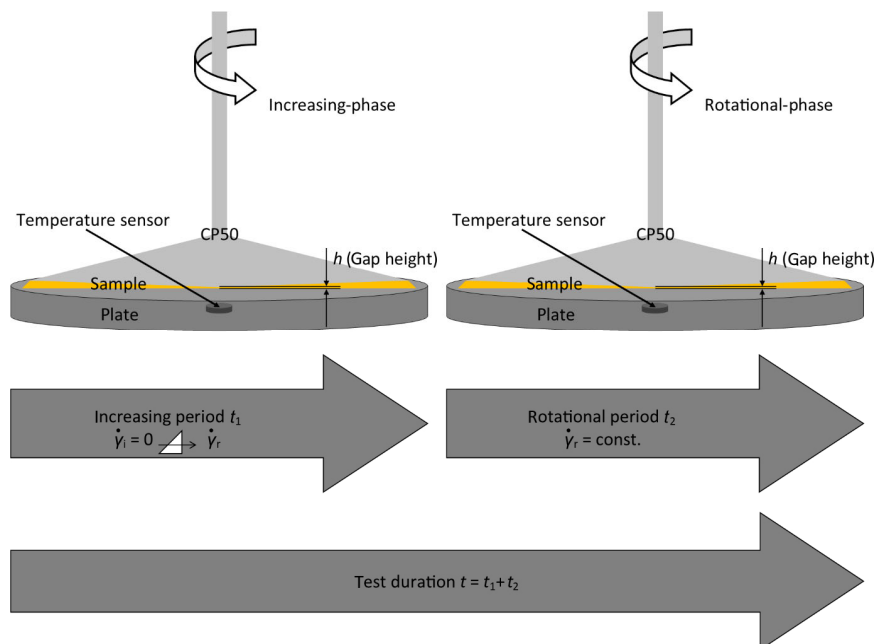


Fig. 1 Schematic illustration of the experimental procedure.

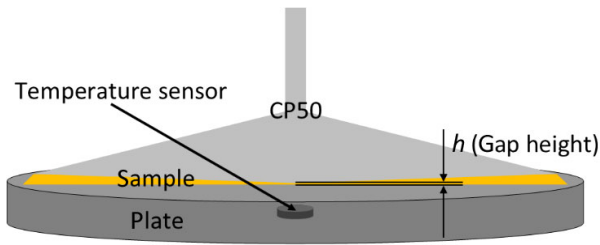


Fig. 2 Schematic of standard plate PTD with the temperature sensor.

located in the centre and just below the bottom plate, recording the average temperature of the grease sample. The PTD measuring cell from Anton Paar has been thoroughly tested in various tests concerning its temperature behaviour. Before the first measurements, the temperature measuring cell was calibrated according to the Anton Paar standard procedure.

Secondly, a new measuring cell, called Calidus, was developed for such purposes, which is installed in an Anton Paar MCR302 rheometer (Fig. 3). Calidus is a modular measuring cell in which different modules can be coupled using a thread system. The temperature module consists of a thermoplastic base plate on which two temperature sensors are mounted (in the centre and slightly off-centre). The Calidus measuring system was also tested and calibrated in advance with a customised test set-up.

Each configuration was supplemented with an Anton Paar environmental control chamber (bonnet) and a PT-100 sensor to record the room temperature during all measurements. This chamber encapsulates

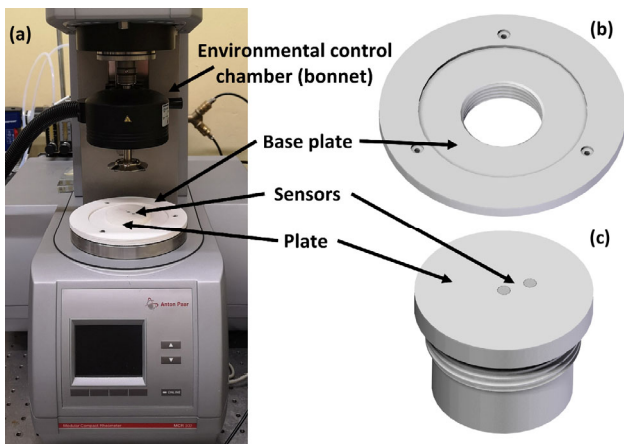


Fig. 3 (a) Calidus coupled to the rheometer; (b) schematic of Calidus base plate; and (c) schematic of Calidus plate with two sensors.

the environment around the sample, minimising heat loss and achieving a more accurate resolution for the temperature measurements.

3 Results and discussion

3.1 Density and the specific heat capacities of lubricating greases studied

The density and the specific heat capacities of the respective greases were required to determine an approachable theoretical temperature curve of the lubricating greases. The density was needed to determine the grease mass considering the respective volume, and the specific heat capacities were needed for the energetic theoretical approach.

Due to the complexity of experimentally measuring the specific densities of such highly viscous materials, theoretical values were determined by Eq. (1) to validate the experimental values.

$$\rho_{\text{grease}} = \rho_{\text{thickener}} \cdot \text{percentage}_{\text{thickener}} + \rho_{\text{baseoil}} \cdot \text{percentage}_{\text{baseoil}} \quad (1)$$

The specific densities of each grease's components required for this purpose can be found in Table 3.

Table 4 shows the theoretical and experimental specific densities and the specific heat capacities of all lubricating greases tested. As can be appreciated, the experimental results agree with the theoretical ones. All experimental values are within a variation range of minus 5% of the theoretical specific density values, except for grease C7 below 10%. Thus, experimental values of specific density were preferred for the following calculations.

It is worth mentioning that the grease's specific densities mainly depend on the base oil's specific density. Thus, conventional greases C1 and C5 have the highest specific density values due to the castor oil used. They are followed in order by grease C4, with mineral oil, and the other greases with PAO (C2, C3, C6, and C7). On the other hand, calcium soap has the highest specific density values among the thickeners, followed by lithium soap and polyurea. The grease with the polyurea-based thickener (1.33 g/cm³), C7, only falls somewhat out of order since the combination with the PAO base oil (0.85 g/cm³) ensures

Table 3 Specific densities at 20 °C of the different grease components.

Ingredient	Specific density (g/cm ³) at 20 °C	Ingredient	Specific density (g/cm ³) at 20 °C
Lithium 12-hydroxystearate	1.03 [28]	Glyceryl monooleate	0.94 [29]
Calcium 12-hydroxystearate	1.08 [30]	Polyhydroxybutyrate	1.22 [31]
Urea	1.33 [32]	Ethyl cellulose	1.14 [33]
Castor oil	0.97 [34]	Beeswax	0.97 [35]
PAO	0.85 [36]	HOSO	0.92 [37]
Mineral oil	0.90 [36]	MTC oil	0.96 [38]
Cellulose	1.50 [39]	Glycerol monostearate	1.03 [40]
Glycerol	1.26 [41]	Cetyl alcohol	0.82 [42]

Table 4 Specific densities (experimentally and theoretically) and specific heat capacity at 20 °C of the different greases used.

Lubricating grease	Experimental specific density (g/cm ³)	Theoretical specific density (g/cm ³)	Specific heat capacity (J/(g·K))
C1	0.9357	0.9780	2.106
C2	0.8126	0.8691	1.948
C3	0.8299	0.8734	2.000
C4	0.8639	0.9124	1.847
C5	0.9481	0.9789	2.206
C6	0.8609	0.9024	2.063
C7	0.8498	0.9441	1.997
B1	1.2109	1.2318	2.245
B2	0.9643	0.9849	2.012
B3	0.9205	0.9414	2.144

a comparatively lower density. In addition, it was found that the specific heat capacities of conventional greases studied were related to their specific density values, such as the higher the specific density was, the higher the heat capacity. Concerning the bio-greases, a similar picture appears, at least about the specific densities. Grease B3, with glycerine and glyceryl monooleate, showed the highest specific density. The grease-specific densities mainly depend on the base oil's specific density; however, the order of the specific heat capacities differs. The grease with the lowest density (B3) is placed between the grease with the highest density (B1) and the medium density (B2). Figure 4 shows an overview of the results obtained.

3.2 Internal temperature changes profile under controlled shear stress conditions

Ahme et al. [43] pointed out that macroscopic structural degradation occurs in lubricating grease during

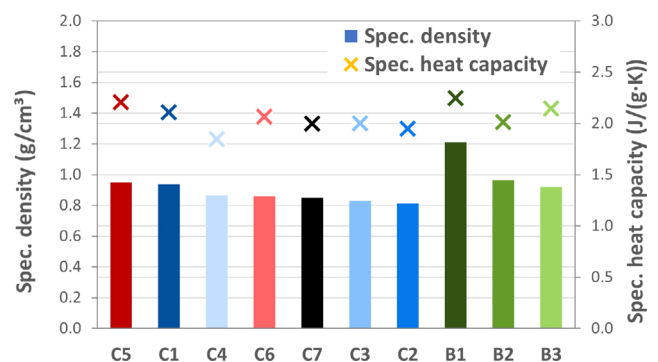


Fig. 4 Comparison of the specific density and the specific heat capacity at a temperature of 20 °C of all investigated lubricating greases.

shearing. Such an increase in the grease's internal temperature may be detected. This research analysed temperature changes inside the bulk of lubricating greases under controlled shear stress conditions at 250 and 500 s⁻¹. Slight differences were observed in grease temperature profiles at 250 s⁻¹ compared to 500 s⁻¹.

The temperature values at 250 s^{-1} were c.a. $1/3$ smaller than those at 500 s^{-1} ; maximum temperature change values between 1.2 and 1.8 K were appreciated for 250 s^{-1} and 1.4–3.2 K for 500 s^{-1} . Thus, for the sake of simplicity, data at 250 s^{-1} were not plotted. Figure 5 shows the shear stress curve and grease temperature within the gap for the lithium grease (C4), which was measured using the standard PTD cell for 22 h (red and light blue, respectively); the room temperature (dark blue) along the test was included. An environmental control chamber (bonnet) was used to mitigate the external heat dissipation.

Figure 5 shows the grease's internal temperature and the internal friction energy during the shearing process. It is essential to realise that the temperature variation within the gap was unaffected by oscillations in the room temperature, as it was kept constant during the entire measurement period. The temperature of stressed grease C4 sharply increased until $25.5 \text{ }^\circ\text{C}$ within the first hour at 500 s^{-1} . Then, the temperature slightly decreased with time until a steady temperature was reached, c.a. $2 \text{ }^\circ\text{C}$ higher than room temperature. It is worth pointing out that the maximum temperature was reached around 1.5 h after the stress overshoot was surpassed due to the low heat transfer rate within the so viscous sample [44].

Before comparing the temperature profiles of the group of lubricating greases studied, adjusting the temperature changes (ΔT) in each test was necessary. For this purpose, it considered a temperature offset

in each test. It was mandatory because the starting grease temperature was neither at room temperature nor the same in the different tests. Therefore, a reference state was necessary to counterbalance the temperature deviations and compare suitable temperature changes along each test. Thus, and considering room temperatures were always the same, the starting temperature value (T_0) was always subtracted from all other measured temperature values (T_i) in each test, according to Eq. (2):

$$\Delta T_i = T_i - T_0 \quad i = 1, \dots, 5,320 \quad (2)$$

The temperature changes (ΔT) determined experimentally at a shear rate of 500 s^{-1} with the standard PTD measuring cell are shown in Figs. 6–8. Figure 6 summarises all conventional greases (lithium, calcium, and polyurea) studied, while Fig. 8 shows the pure biogenic greases. The grease C6 is missing in Fig. 6 because it showed a high shear rate fracture phenomenon, and no reproducible data were obtained. Three fresh samples were measured for each grease; the corresponding average values are shown in Fig. 6.

As can be observed in Fig. 6, the temperature change profiles present the next evolution: A sudden rise in temperature change caused by the solid internal friction due to a high structural consistency of the lubricating grease and a more or less smooth drop until reaching a stationary value of the ΔT , once the grease structural degradation reached a steady

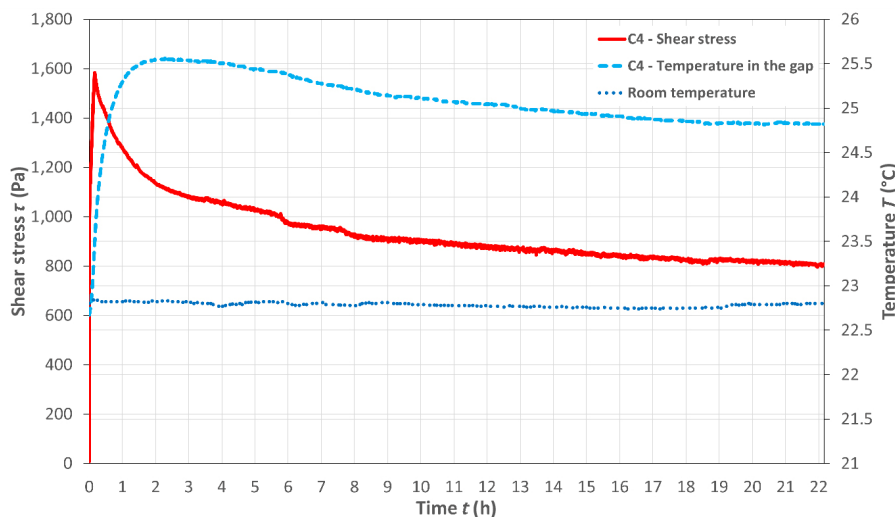


Fig. 5 Experimental room temperature, shear stress, and temperature profile of lithium grease C4, with the standard PTD measuring cell at a shear rate of 500 s^{-1} .

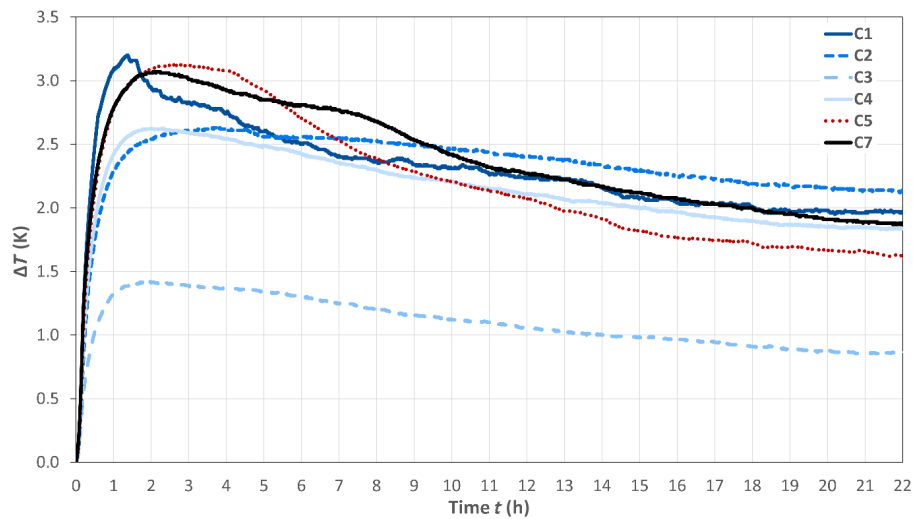


Fig. 6 Experimental temperature profile of conventional lubricating greases, with the standard PTD measuring cell at a shear rate of 500 s^{-1} .

state. All conventional greases reached their maximum temperature change within the first 4 h (240 min), being the limit time values of 72 and 240 min for greases C1 and C2, respectively. Grease C1 showed the highest value of the maximum ΔT among all conventional greases, c.a. 3.2 K, while grease C3 showed the lowest temperature change, c.a. 1.4 K. It is noticeable that greases C2 and C3, formulated with PAO and lithium soap, developed a similar temperature change profile, characterized by a moderate increase until the maximum ΔT value, followed by a smooth decay till a steady temperature change was reached. Much higher temperature changes were detected for grease C2 than C3, probably due to its base oil's higher viscosity, which hampers heat dissipation with the environment. Furthermore, the grease C1 showed the sharpest increase at the beginning of the test, after which the curve roughly dropped to a slowly decreasing course after eight hours. The highly entangled structural skeleton achieved by the highest lithium soap content [21] might bring the highest internal friction during the shearing process, which led to this drastic temperature increase in the bulk grease. Despite greases C2 and C4 being formulated with different base oils, they showed similar temperature change profiles. Both had similar lithium soap content and the same base oil's kinematic viscosity. In general, it can be said that lithium greases, except for C1, showed a softer temperature variation along the test. Calcium grease C5 shows the second sudden rise in

temperature change and a steep decay until the steady value of ΔT is reached. Moreover, this grease suffered the highest temperature variation once the maximum temperature reached 1.5 K. While polyurea grease (C7) showed a temperature change profile similar to lithium grease with the highest soap content (C1).

In addition, it can be stated that if one looks at the individual composition of these lubricating greases, the ones with castor base oil showed a substantial increase in internal temperature change and then a strong decay. Therefore, the main component of the lubricating grease, i.e., the base oil, decisively determines its properties. Furthermore, it was appreciated that the grease's specific densities and heat capacities might be involved in the internal temperature change once the maximum value was reached. Thus, greases with castor oil (greases C1 and C5), which has both the highest specific densities and heat capacities, showed a substantial increase. They then showed a strong decay of internal ΔT . The combination of polyurea with a PAO (grease C7) also showed these characteristics of internal thermal behaviour, despite its lower values of specific density and heat capacity. In contrast, the greases with a lithium thickener and a PAO (greases C2 and C3) or mineral oil (grease C4), which has lower specific densities and heat capacities, showed a lower increase in internal temperature change and a smooth drop of the ΔT until the steady value was reached. Finally, it

is worth pointing out that grease C6, with the highest soap content, showed the highest temperature change, c.a. 4.56 K. After that, grease C6 was rejected from the measured geometry due to the fracture phenomenon at this high shear rate, and no reproducible data could be shown. In fact, according to Ahme et al. [44], this agglomerate-based calcium grease structure was highly affected by the stressing conditions tested.

These temperature change profiles have been related to the expended energy on structural degradation of lubricating grease during the shearing process published by Ahme et al. [44] (Fig. 7). It was appreciated that the larger the ratio of expended energies (R_{tee}) is, the lower the temperature changes (ΔT) are. In other words, samples that showed the lowest structural degradation in the stressed greases (C2, C3, and C4) developed the lowest temperature changes. Contrarily, the greases (C1, C5, and C7) with the lowest R_{tee} values, which means more structural degradation in the stressed grease [44], had the highest temperature change along the test. It was evidenced by the highest maximum ΔT and the steepest drops until reaching the steady value of ΔT . Therefore, a direct relationship was found between structural degradation (inverse of R_{tee}) and the temperature changes in the stressed grease. It is worth pointing out that base oil viscosity played a crucial role in the dissipation of this internal temperature increase. Thus, although the grease C3 had a similar R_{tee} value to greases C4 or C2, it showed a temperature change c.a. 52% lower than these greases.

Concerning pure biogenic greases studied (Fig. 8), biogenic greases B2 and B3 showed a similar temperature change profile to the conventional greases

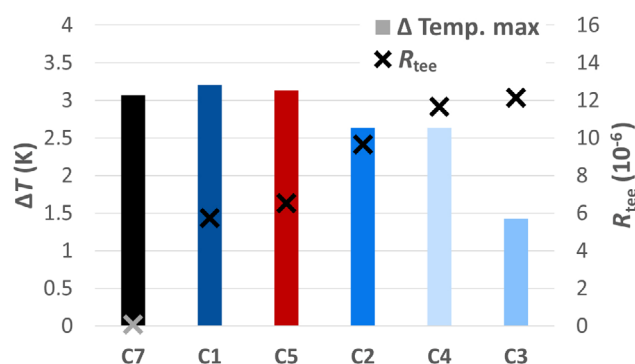


Fig. 7 Comparison of the maximum ΔT values with the ratio of expended energies (R_{tee}).

studied, characterized by a moderate increase until the maximum ΔT value, followed by a smooth decay till a steady temperature change was reached. Thus, greases B2 and B3 reached the maximum ΔT at 300 and 102 min, respectively. It is noteworthy that grease B2 showed the most remarkable temperature change in the group of pure biogenic greases, obtaining the highest ΔT , c.a. 3.2 K, while grease B3 was the lowest, c.a. 1.6 K. On the other hand, the grease B1 developed an atypical course of ΔT profile. It means this grease did not reach a maximum temperature value within the test period; the temperature increases linearly to 2.6 K after 22 h. It could be because the thickener consists of cellulose fibers, which are quite strong and do not end up breaking, but instead, move and rub against each other. This phenomenon produces a continuous temperature increase due to significant internal friction.

In contrast to the analysed conventional greases, there is no discernible trend in the specific thermal capacities. Therefore, it can be concluded that the thickener types used in this work react to tribological stress with different heat development regarding typical friction and wear mechanisms.

3.3 Temperature measurements using Calidus cell

The Calidus measuring cell comprised two sensors to measure a temperature difference within the bulk of grease with a plate–plate measuring system (see Fig. 3). A cone–plate measuring system was used, for which the shear rate was the same in the entire measuring gap. Due to this condition, the sensor's temperature differed slightly (between 0.1 to 0.2 K), which was within the range of measurement accuracy. Therefore, an average value was calculated from both temperature sensors.

It should be mentioned that some differences in roughness were appreciated with the surfaces in each temperature-measuring cell. The surface in the conventional PTD cell was titanium ($R_z = 5.417$), and a polylactide-based polyester in the Calidus cell ($R_z = 27.704$). These differences hardly affected most of the shear stress profiles measured at such a high shear rate with the prototype of the new Calidus temperature measuring cell in relation to the conventional PTD cell. Unfortunately, the shear stress fell to 0 after

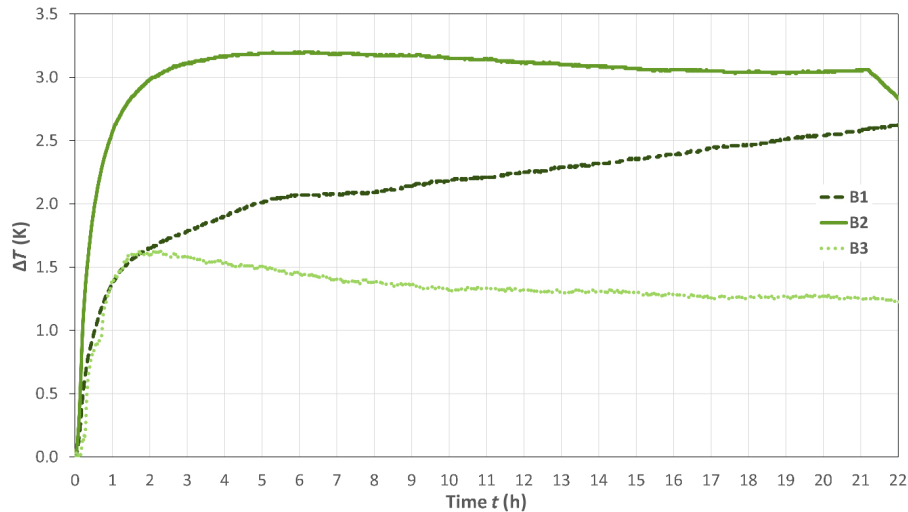


Fig. 8 Experimental temperature profile of the pure biogenic lubricating greases, with the standard PTD measuring cell at a shear rate of 500 s^{-1} .

about 2 h due to some greases leaking out of the measuring gap. Therefore, the surface of the Calidus measuring cell had higher surface roughness, which may promote the fracture and the ejection of the sample from the gap at a high shear rate [26, 45].

Taking into account the previous results published by Ahme et al. [44], the type of structural pattern related to the type of thickener higher affects the internal frictional energy involved in the grease degradation process than both the thickener content and the oil viscosity. Consequently, only the optimal data for the selected lithium-(C2), calcium-(C5), polyurethane-(C7), and pure bionic-(B2) greases were considered to analyse the results with the newly developed Calidus temperature measuring cell. Figure 9 shows the experimental temperature changes of these selected greases during 22 h at a shear rate of 500 s^{-1} using both temperature-measuring cells. The newly developed Calidus temperature measuring cell results are represented with a dotted line and those of the conventional PTD cell with a solid line.

As can be appreciated in Fig. 9, the temperature profiles obtained by both devices are essentially similar, only differ more significantly in the case of grease C5. The temperature changes measured by either method are affected by the extremely high viscosity of these greases. The Calidus device has different mass inertia of the measuring cell material, and the sensors installed have different thermal

conductivities concerning their inertia due to the better installation position (see Fig. 3). Consequently, the temperature-change values determined with Calidus are higher than those of the PTD measuring cell. Moreover, the maximum ΔT values were detected faster with the Calidus cell. It leads to the conclusion that the Calidus-based temperature measurement was more thorough since it was placed almost touching the grease and not just below the bottom plate like the PTD device. Thus, the conventional PTD configuration led to the average temperature of the grease bulk, while the Calidus cell showed the local temperature inside the gap. In summary, the new Calidus measuring cell delivers accurate results regarding temperature values, which are close to those of the PTD measuring cell. By further developing the surface roughness of the Calidus measuring cell, it will be qualified for reliable rheological measurements in the future.

3.4 Theoretical approach to a temperature determination

A theoretical approach to the grease temperature within the measuring gap was made in this work. This approach is understood as a theoretical temperature determination and is not intended to represent a model. Instead, it should compare the experimental observations and the theoretical predictions and help validate the results obtained.

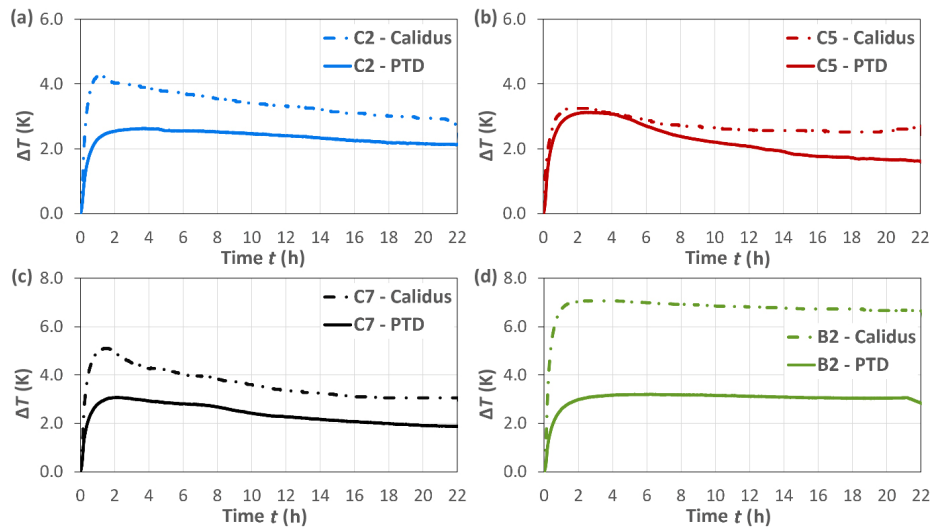


Fig. 9 Comparison of the temperature measuring cell–Calidus and Anton Paar PTD–with the selected lubricating greases (a) C2; (b) C5; (c) C7; and (d) B2 concerning the experimental ΔT profile.

Although it was mainly based on the 1st Law of Thermodynamics, the heat transfer rate into the grease was not considered:

$$Q_{12} + W_{12} = U_1 - U_2 \tag{3}$$

with

Q_{12} = quantity of energy supplied to the system as heat (J);

W_{12} = amount of thermodynamic work done by the system (J);

$U_1 - U_2$ = change in the internal energy of a closed system (J).

This approach assumed that the system did not exchange heat with the environment. The exchange of thermal energy with the environment cannot be prevented entirely, although an environmental control chamber (bonnet) was used. Therefore, it was defined as

$$Q_{12} = 0 \tag{3.1}$$

Thus, it was stated that

$$W_{12} = U_1 - U_2 = m_i \cdot c_i \cdot (T_1 - T_2) \tag{3.2}$$

with

Q_{12} = quantity of energy supplied to the system as heat (J);

W_{12} = amount of thermodynamic work done by the system (J);

$U_1 - U_2$ = change in the internal energy of a closed system (J);

m_i = sample mass (g);

c_{pi} = sample specific heat capacity (J/(g·K));

$(T_1 - T_2)$ = sample temperature change (K).

Rearranging according to T results in

$$\Delta T = \frac{W_{12}}{m_i \cdot c_{pi}} = (K) \tag{3.3}$$

where

$$m_i = \rho_i \cdot v_i = (g) \tag{3.4}$$

and

$$W_{12} = W_R = \int_0^{15} \frac{M_d \cdot n \cdot 2\pi}{60} dt = \frac{M_d \cdot n \cdot \pi}{2} = (J) \tag{3.5}$$

While using Eq. (3.3), it is then possible to easily determine the respective theoretical temperature change value for each measuring point of the investigation. Of course, the theoretically determined temperature curves should not prove the experimentally determined temperature curves but rather help to evaluate the results better. Thus, Fig. 10 shows the experimental data of selected greases obtained by the standard PTD cell (solid line) and the Calidus cell (dashed line) at a shear rate of 500 s⁻¹ for 22 h and the theoretical values calculated by Eq. (3.3) (dashed line).

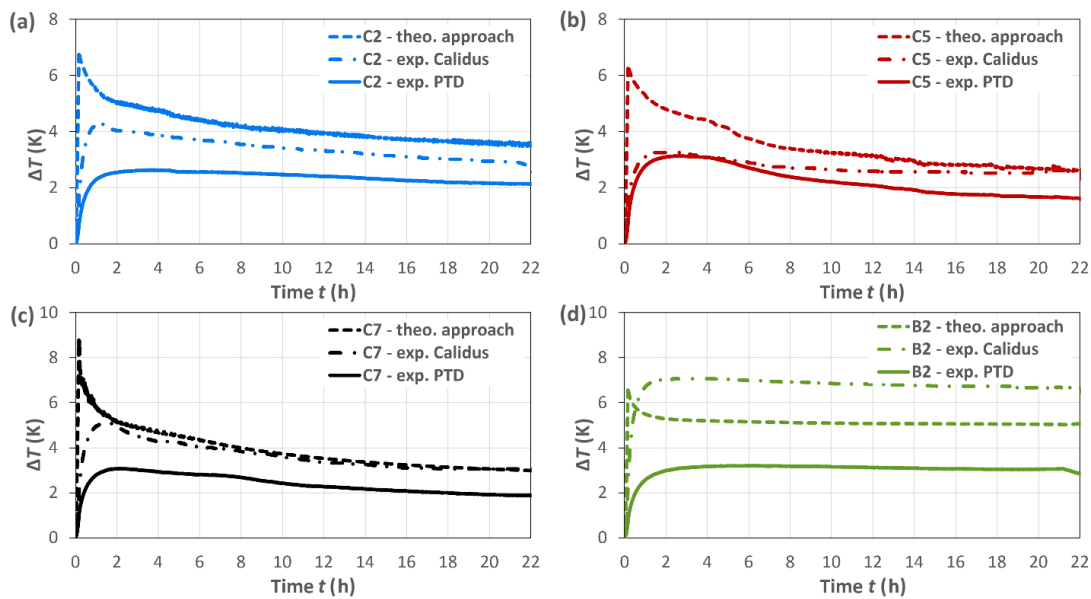


Fig. 10 Comparison of the rheometer measuring Cell–Calidus and Anton Paar PTD—with the use of lubricating greases (a) C2; (b) C5; (c) C7; and (d) B2 concerning the experimental ΔT profile and the theoretical approach curve.

It should be emphasised that the values determined with the theoretical approach were consistently higher than the experimentally determined values. Only in the case of the pure biogenic grease B2, the Calidus measurement curve is above the theoretical prediction. The theoretical approach strictly followed the shear stress curve, meaning that the grease heat transfer rate was irrelevant in most of the shearing time in the experimental data. However, more significant deviations were mainly observed at the beginning of the test, i.e., the greases showed the most significant deviations up to about 1.5 h between the experimental and theoretical data. It was expected since the extremely low grease thermal conductivity and high viscosity of all greases studied (NLGI grade 2). Nevertheless, from 6 h onwards, this simple theoretical approach describes a similar temperature change profile to the two experimentally determined ones, again except for the organic grease B2. In addition, the determined temperature values of Calidus are closer to the theoretical prediction.

4 Conclusions

This work has evidenced a relationship between the structural degradation and the temperature changes associated with the stressed grease at a high shear

rate for several conventional model greases. They all belong to NLGI grade 2 and a group of newly developed pure biogenic greases (with lower NLGI grade). All greases showed an internal temperature profile characterized by a sudden rise in ΔT , caused by the strong internal friction due to a high structural consistency of the lubricating grease. A subsequent ΔT decay followed it until it reached the steady state value. In addition, based on the knowledge gained in this work, a new measuring system called Calidus has been developed. Finally, a straightforward theoretical approach was proposed for calculating the temperature change of stressed greases.

The examined conventional model greases showed significant differences in the temperature profiles—the grease C1, with a thickener content of 16.1 wt%, heated up the most (3.2 K) and showed a drastic drop of ΔT . The grease C5, with a content of 9.7 wt% and the same base oil, was slightly below this and on par with the grease C7, with a content of 19.6 wt% and poly-alpha-olefin (PAO) as base oil. It means that it is not the absolute concentration of the thickener that is decisive for the internal frictional heating but the type of thickener and the base oil. These three greases showed both the highest specific densities and heat capacities, which evidenced that the specific thermal capacity of these greases may be involved in the

temperature change profile. Thus, grease C5, with the more significant decay of ΔT , had the highest specific thermal capacity, followed by greases C1 and C7. In contrast, grease C4, with the lowest value of specific thermal capacity, showed a smooth drop of the ΔT until the steady value was reached.

On the other hand, a direct relationship was found between structural degradation (inverse of R_{tee}) and the temperature changes in the stressed greases. Thus, the larger the ratio of expended energies (R_{tee}), the lowest the temperature change (ΔT). Therefore, samples that showed the lowest structural degradation in the stressed grease (C2, C3, and C4) developed the lowest temperature changes. Contrarily, the greases (C1, C5, C7) with the lowest R_{tee} values had the highest maximum ΔT and the steepest drops until reaching the steady value of ΔT . It is worth pointing out that base oil viscosity played a crucial role in the dissipation of this internal temperature increase. Thus, the grease C3, with 13 wt% of Li-soap but the lowest base oil's viscosity, despite having a similar R_{tee} value than greases C4 or C2, showed a temperature change c.a. 52% lower than these greases. In addition, grease C3 showed the lowest maximum ΔT , and the temperature profile was characterized by a moderate variation of ΔT along the test.

Regarding the measurements with Calidus, it can be stated that the measurements with this newly developed measuring cell are more precise, as the mass inertia of the measuring cell material (Calidus: polylactide, PTD: titanium) is lower, and therefore, the temperature values are reached faster. At the same time, the sensors used with Calidus have a better installation position and are thus located directly at the measuring gap. Nevertheless, it should be mentioned that the surface finish should be optimised for future measurements. In addition, Calidus's experimental data correlated much better with the theoretical approach. The theoretically determined temperature values were consistently higher than the experimentally determined ones. It is plausible because $Q_{12} = 0$ was assumed in the calculation. If future investigations make it possible to determine a theoretical value for Q_{12} , this could bring the theoretical model closer to reality. Subsequently, with a more extensive base of experimental results, which also considers the heat transfer rate within the grease,

the theoretical model could be further developed to determine temperature values as input variables without experimental temperature measurements.

Declaration of competing interest

The authors have no competing interests to declare that are relevant to the content of this article.

Electronic Supplementary Material: Supplementary material of an image with a thermal imaging camera, and further diagrams of the experimental temperature changes are available in the online version of this article at <https://doi.org/10.1007/s40544-023-0818-7>.

Open Access This article is licensed under a Creative Commons Attribution 4.0 International License, which permits use, sharing, adaptation, distribution and reproduction in any medium or format, as long as you give appropriate credit to the original author(s) and the source, provide a link to the Creative Commons licence, and indicate if changes were made.

The images or other third party material in this article are included in the article's Creative Commons licence, unless indicated otherwise in a credit line to the material. If material is not included in the article's Creative Commons licence and your intended use is not permitted by statutory regulation or exceeds the permitted use, you will need to obtain permission directly from the copyright holder.

To view a copy of this licence, visit <http://creativecommons.org/licenses/by/4.0/>.

References

- [1] Dresel W, Heckler R P. Lubricating Grease. In: *Lubricants and Lubrication, 2nd Ed.* Mang T, Dresel W, Eds. Weinheim: Wiley-VCH, 2007: 603–646.
- [2] Kuhn E. *Zur Tribologie der Schmierfette: Eine energetische Betrachtungsweise des Reibungs- und Verschleißprozesses*, 2nd ed. Renningen: expert Verlag, 2017 (in German).
- [3] Bartz W J. *Schmierfette: Zusammensetzung, Eigenschaften, Prüfung und Anwendung*. Renningen-Malmsheim: expert-Verl., 2000 (in German).
- [4] Paszkowski M. Assessment of the effect of temperature, shear rate and thickener content on the thixotropy of lithium

- lubricating greases. *Proc Inst Mech Eng Part J* **227**(3): 209–219 (2013)
- [5] Sánchez R, Valencia C, Franco J M. Rheological and tribological characteriza-tion of a new acylated chitosan-based biodegradable lubricating grease: A compara-tive study with traditional lithium and calcium greases. *Tribol Trans* **57**(3): 445–454 (2014)
- [6] Rezasoltani A, Khonsari M M. On the correlation between mechanical degrada-tion of lubricating grease and entropy. *Tribol Lett* **56**(2): 197–204 (2014)
- [7] Zhou Y. On the mechanical ageing of lubricating greases. Ph.D. Thesis. Beijing (China): University of Twente, 2018.
- [8] Delgado M A, Franco J M, Kuhn E. Effect of rheological behaviour of lithium greases on the friction process. *Ind Lubr Tribol* **60**(1): 37–45 (2008)
- [9] Kuhn E. Correlation between system entropy and structural changes in lubricating grease. *Lubricants* **3**(2): 332–345 (2015)
- [10] Kuhn E. Application of a thermodynamic concept for the analysis of structural degradation of soap thickened lubricating greases. *Lubricants* **6**(1): 7 (2018)
- [11] Kuhn E. Experimental grease investigations from an energy point of view. *Ind Lubr Tribol* **51**(5): 246–251 (1999)
- [12] Osara J, Bryant M. Thermodynamics of grease degradation. *Tribol Int* **137**: 433–445 (2019)
- [13] Rezasoltani A, Khonsari M. An engineering model to estimate consistency reduction of lubricating grease sub-jected to mechanical degradation under shear. *Tribol Int* **103**: 465–474 (2016)
- [14] Bryant M, Khonsari M, Ling F. On the thermodynamics of degradation. *Proc R Soc A* **464**: 2001–2014 (2008)
- [15] Kuhn E. Tribological stress of lubricating greases in the light of system entropy. *Lubricants* **4**(4): 37 (2016)
- [16] Adhvaryu A, Sung C, Erhan S Z. Fatty acids and antioxidant effects on grease microstructures. *Ind Crops Prod* **21**(3): 285–291 (2004)
- [17] Delgado M, Valencia C, Sánchez M C, Franco J, Gallegos C. Fatty acids and antioxidant effects on grease microstructures. *Tribol Lett* **23**: 47–54 (2006)
- [18] Pan J, Yanhai C, Yang J. Effect of Heat treatment on lubricating properties of lithium lubricating grease. *RSC Adv* **5**: 58686–58693 (2015)
- [19] Osara J, Bryant M. A temperature-only system degradation analysis based on thermal entropy and the degradation-entropy generation methodology. *Int J Heat Mass Transfer* **158**: 120051 (2020)
- [20] Zhou Y, Bosman R, Lugt P. A master curve for the shear degradation of lubricating greases with a fibrous structure. *Tribol Trans* **62**: 1–21 (2018)
- [21] Delgado M A, Valencia C, Sánchez M C, Franco J M, Gallegos C. Influence of soap concentration and oil viscosity on the rheology and microstructure of lubricating greases. *Ind Eng Chem Res* **45**(6): 1902–1910 (2006)
- [22] Acar N, Kuhn E, Franco J M. Tribological and rheological characterization of new completely biogenic lubricating greases: A comparative experimental investigation. *Lubricants* **6**(2): 45 (2018)
- [23] Acar N, Franco J M, Kuhn E, Gonçalves D E P, Seabra J H O. Tribological investigation on the friction and wear behaviors of biogenic lubricating greases in steel–steel contact. *Appl Sci* **10**(4): 1477 (2020)
- [24] NETZSCH-Gerätebau GmbH, Precise determination of the specific heat capacity by means of DSC on <https://www.netzsch-thermal-analysis.com/en/contract-testing/tips-tricks/dsc/precise-determination-of-the-specific-heat-by-means-of-dsc/>, 2022.
- [25] NETZSCH-Gerätebau GmbH, Specific heat capacity (cp), on <https://www.netzsch-thermal-analysis.com/en/contract-testing/glossary/specific-heat-capacity-cp/>, 2022.
- [26] Delgado M A, Secouard S, Valencia C, Franco J M. On the steady-state flow and yielding behaviour of lubricating greases. *Fluids* **4**(1): 1477 (2019)
- [27] Deutsches Institut für Normung. DIN 51810 *Prüfung von Schmierstoffen-Prüfung der rheologischen Eigenschaften von Schmierfetten: Teil 1: Bestimmung der Scherviskosität mit dem Rotationsviskosimeter und dem Messsystem Kegel/Platte*. Beuth, 2017 (in German), on <https://www.beuth.de/de/norm/din-51810-1/269916043>.
- [28] European Chemicals Agency, Lithium stearate: Density on: <https://echa.europa.eu/es/registration-dossier/-/registered-dossier/22040/4/5>, 2022.
- [29] PubChem, Glyceryl monooleate: Density, on <https://pubchem.ncbi.nlm.nih.gov/compound/Glyceryl-monooleate#section=Solubility>, 2022.
- [30] European Chemicals Agency, fatty acids, tallow, calcium salts: density, on <https://echa.europa.eu/es/registration-dossier/-/registered-dossier/5720/4/5>, 2022.
- [31] Polymer Properties Database, Polyhydroxybutyrate: Density, on <https://polymerdatabase.com/polymers/poly3-hydroxybutyrate.html>, 2022.
- [32] European Chemicals Agency, Urea: Density, on <https://echa.europa.eu/de/registration-dossier/-/registered-dossier/16152/4/5>, 2022.
- [33] Chemical Book, Ethyl cellulose: Density, on https://www.chemicalbook.com/ChemicalProductProperty_EN_CB6165620.htm, 2022.
- [34] European Chemicals Agency, Castor oil: Density, on <https://echa.europa.eu/de/registration-dossier/-/registered-dossier/14599/4/5>, 2022.



- [35] Tinto W F, Eluffoye T O, Roach J. Chapter 22-Waxes. In: *Pharmacognosy*. Badal S, Delgoda R, Eds. Boston: Academic Press, 2017: 443–455.
- [36] OKS Spezialschmierstoffe GmbH, oils with high-performance additives for reliable lubrication: properties of base oils, on <https://www.oks-germany.com/en/tribology/types-of-lubricants/oils/>, 2022.
- [37] AMD Special Oil LLC, Sunflower Oil, High Oleic RBDW: Density, on <https://www.amdoilsales.com/products/hosunflower/>, 2022.
- [38] Kraft Chemical, Safety Data Sheet MTC oil: Density, on <https://greenfield.com/wp-content/uploads/2018/11/MCT-Oil-SDS.pdf>, 2022.
- [39] PubChem, Cellulose: Density, on <https://pubchem.ncbi.nlm.nih.gov/compound/CELLULOSE>, 2022.
- [40] Wikipedia, Glycerol monostearate: Density, on https://en.wikipedia.org/wiki/Glycerol_monostearate, 2022.
- [41] PubChem, Glycerol: Density, on <https://pubchem.ncbi.nlm.nih.gov/compound/Glycerol#section=Density>, 2022.
- [42] PubChem, 1-Hexadecanol (Cetyl alcohol): Density, on <https://pubchem.ncbi.nlm.nih.gov/compound/1-Hexadecanol#section=Density>, 2022.
- [43] Ahme L, Kuhn E, Delgado Canto M Á. Experimental study on the expended energy on structural degradation of lubricating greases. *Tribol lett* **70**(3): 81(2022)
- [44] Wu L, Tan Q. A study of cooling system in a grease-lubricated precision spindle. *Adv Mech Eng* **8**(8): 1687814016665296 (2016)
- [45] Balan C, Franco J M. Influence of the geometry on the transient and steady flow of lubricating greases. *Tribol Trans* **44**(1): 53–58 (2001)



Leif AHME. He completed his Bachelor of Engineering degree in 2015 and earned his Master of Science degree in 2017, both in Mechanical Engineering from Hamburg University of Applied Sciences in Hamburg, Germany.



Erik KUHN. He reached his Dr.-Ing. degree in 1987 at Otto von Guericke University in Magdeburg, Germany. Since 1991, he has been a full Professor at Hamburg University of

Subsequently, he embarked as a Ph.D. candidate in collaboration with the Tribology Research Center of the Hamburg University of Applied Sciences and the University of Huelva. His research expertise centres on the field of Tribology, explicitly focusing on the intricate study of structural degradation in lubricating greases.

Applied Sciences (HAW) and head of the Tribology Research Center. His research area is Tribology of lubricating greases, and he is the author of a book with the same title. Prof. KUHN is the organizer of the annual Arnold Tross Colloquium.



Miguel Ángel DELGADO. He received his M.Eng. (2000) and Ph.D. (2005) degrees in Chemical Engineering from the University of Huelva, Spain. He joined the Centre for Research in Product Technology and Chemical Processes (Pro2TecS)

in 2011. His current position is as a Professor at the Department of Chemical Engineering at the same institution. His research areas cover the manufacture and rheological and microstructural characterization of bio-thickener-based lubricating greases and vegetable oils. Nowadays, he is very involved in electro-active control of the friction process.